

## Reaction and Kinetic Studies of Immobilized Enzyme Systems: Part-I Without External Mass Transfer Resistance

M. Sivakumar<sup>1</sup>, R. Senthamarai<sup>2,\*</sup>, L. Rajendran<sup>3</sup>, M.E.G. Lyons<sup>4</sup>

<sup>1</sup> Department of Mathematics, College of Science and Humanities, SRM Institute of Science and Technology, Vadapalani, Chennai, India.

<sup>2</sup> Department of Mathematics, College of Engineering and Technology, SRM Institute of Science and Technology, Kattankulathur – 603 203, Tamilnadu, India.

<sup>3</sup> Department of Mathematics, Academy of Maritime Education and Training (AMET) Deemed to be University, India.

<sup>4</sup> School of Chemistry & AMBER National Centre, University of Dublin, Trinity College Dublin, Ireland

\*E-mail: [senthamr@srmist.edu.in](mailto:senthamr@srmist.edu.in)

Received: 5 March 2022/ Accepted: 26 July 2022 / Published: 10 October 2022

---

In this paper, the nonlinear reaction-diffusion equation is solved analytically for estimating the substrate concentration and effectiveness factor without external mass transfer resistance concerning various geometrical shapes such as planar, cylindrical and spherical forms of pellets used for immobilized enzyme reactions. Taylor's series method is applied to approximate the dimensionless substrate concentration and its overall effectiveness factor on immobilized enzyme reactions. The analytical solution obtained by TSM and the previous analytical results obtained using He's Variational iteration method and the Modified Adomian Decomposition method on the same model are compared with the numerical results (MATLAB software).

---

**Keywords:** Mathematical modeling, Non-linear reaction-diffusion equations, Taylor's series method, Michaelis-Menten kinetics, Immobilized enzyme reactions.

### 1. INTRODUCTION

In view of the purpose of bioreactor design, modeling and simulation and its process development, it is necessary to investigate the intrinsic kinetics for enzymatic reactions. That is reaction kinetics without mass transfer limitations. In immobilization of enzymes, there are several factors which affect the observed kinetics, such as inter-particle and intra-particle diffusion limitations, the partitioning of substrate between the support and bulk of the solution, conformation and spatial effects due to the immobilization mechanism. The consequences of such immobilizations result in

disfiguration of the enzyme and due to which the flux of the substrate may be resisted and concentration levels of the substrate vary. These effects depend on the properties of the support, the substrate and its concentration and on the immobilization procedure [1-3]. The mass transfer limitation effects on the observed reaction rates are due to external mass transfer resistance of substrate from the bulk fluid phase to the external surface of support pellets and internal mass transfer resistances due to pore diffusion [4, 5].

In [6], an optimization algorithm has been applied for the estimation of several substrate mass transfer parameters, including the effective diffusivity of the substrate within the support pellets and the overall external mass transfer coefficient, based on the experimental data under irreversible uni reactant immobilized enzyme systems following Michaelis-Menten mechanism, with some changes in assumptions [7, 8] on the construction of the nonlinear model [9] considered here. Using the kinetic model obtained, as in previous work [10], the mathematical model under consideration has analytically been solved for the dimensionless substrate concentration profile without external mass transfer resistance using He's variational iteration method. Moreover, Krishnan Lakshmi Narayanan has also recently solved the same model [11] using the modified Adomian decomposition method. Weise et al. [12] solved the set of coupled non-linear differential equations in a batch stirred-tank electrochemical reactors numerically using Runge-Kutta method.

In this paper, the model under consideration has been solved for the dimensionless substrate concentration profile using Taylor's series method [13, 14] and the effectiveness factor [9, 15] under various geometrical shapes of the catalyst pellets viz. planar, cylindrical and spherical. Also, the results have been tabulated and shown the variations of the concentration levels graphically for these three cases. The effectiveness factor variations for various values of the parameters have been found and tabulated. Concentration profiles obtained from the three usual methods viz. Taylor's Series method, VIM and MADM have been compared with the numerical results. The overall effectiveness factor has also been found by the two methods, TSM and MADM and compared with the numerical results on the effectiveness factor.

### Nomenclature:

Parameter	Meaning	Unit (Planar)	Unit (Others)
$S$	Substrate Concentration	(kg/m <sup>3</sup> )	(μmol/cm <sup>3</sup> )
$D_e$	Effective diffusivity of the substrate in the pellet	(m <sup>2</sup> /s)	(m <sup>2</sup> /s)
$K_m$	Michaelis-Menten constant	(kg/m <sup>3</sup> )	(μmol/cm <sup>3</sup> )
$v$	Reaction rate	kg/s/m <sup>3</sup> cat	μmol/min/cm <sup>3</sup> cat
$V_m$	Maximum reaction rate	kg/s/m <sup>3</sup> cat	μmol/min/cm <sup>3</sup> cat
$S_b$	Substrate concentration in the bulk fluid phase	(kg/m <sup>3</sup> )	(μmol/cm <sup>3</sup> )
$R$	Half-thickness of the pellet	(m)	(m)
$g$	Pellet shape factor	None	None
$C(X)$	Dimensionless substrate concentration	None	None
$X$	Dimensionless distance to the center or the surface of symmetry of the pellet	None	None

$x$	Distance to the centre	None	None
$\beta$	Dimensionless Michaelis Menten constant $\beta$	None	None
$\alpha$	Thiele Modulus	None	None
$\eta$	Effectiveness Factor	None	None

## 2. MATHEMATICAL FORMULATION OF THE MODEL

The kinetic model for immobilized enzymes has been developed under the following assumptions [6-8]:

1. The kinetics of the immobilized enzymes is described by the Michaelis-Menten equation for irreversible reactions.
2. The enzyme is uniformly attached to the surface of the support material.
3. The partition effect from the bulk fluid phase to the support is neglected.
4. Within the support, temperature and effective diffusivity are constant.
5. Enzyme deactivation is neglected.
6. Steady state conditions are considered.

All enzyme molecules are equally active and substrate diffuses through a thin fluid phase surrounding the support surface to reach the reactive surfaces of adsorbed enzymes, as depicted in Figure 1.

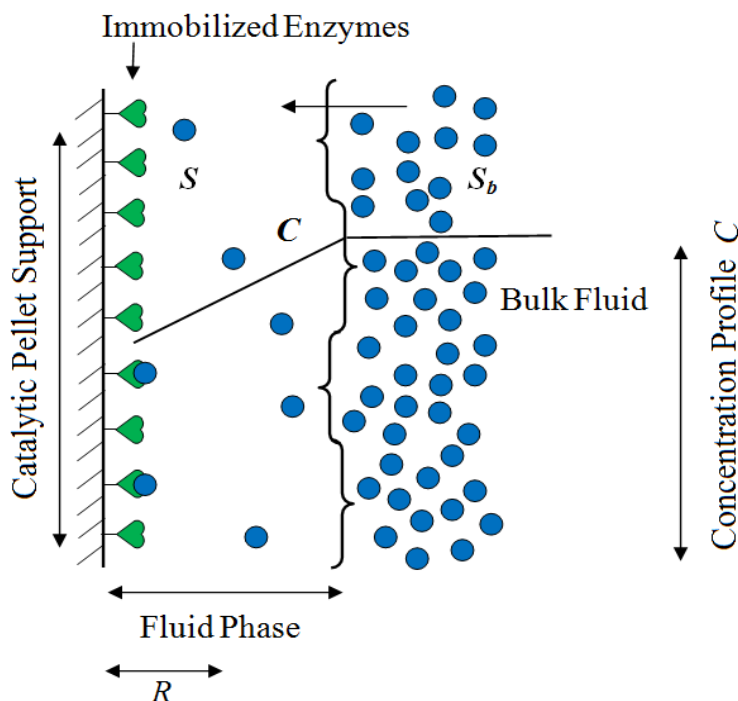


**Figure 1.** Schematic representation of the immobilized enzyme system

According to the substrate concentration dependence of the apparent maximum reaction rate and Michaelis-Menten constant in immobilized enzyme reactions, the one-dimensional non-linear steady state second order equation [9] which describes the enzyme kinetics for the analysis of the substrate concentration variations is given by

$$\frac{d^2S}{dx^2} + \frac{g-1}{x} \frac{dS}{dx} = \frac{V_m S}{K_m D_e \left(1 + \frac{S}{K_m}\right)} \tag{1}$$

which implies that at  $x = 0$ ;  $\frac{dS}{dx} = 0$  (2)

and at  $x = R$ ,  $S = S_b$  (3)

In the above expressions,  $x$  is distance from the pellet surface to the center,  $R$  is the half-thickness of the pellet,  $S$  is the substrate concentration,  $S_b$  is substrate concentration in the bulk fluid phase,  $D_e$  is effective diffusivity of the substrate in the pellet and  $g$  is the pellet shape factor which for slab, cylindrical and spherical pellets is 1, 2 and 3, respectively. Considering the dimensionless parameters [6] defined as

$$C = \frac{S}{S_b}, X = \frac{x}{R}, \beta = \frac{S_b}{K_m} \text{ and } \alpha = R \sqrt{\frac{V_m}{K_m D_e}} \text{ (Thiele Modulus)} \tag{4}$$

where  $X$  is the dimensionless distance to the center or the surface of symmetry of the pellet and  $g$  is the pellet shape factor which for slab, cylindrical and spherical pellets is 1, 2 and 3, respectively, we have the transformed expressions to the dimensionless form as

$$\frac{d^2C}{dX^2} + \frac{g-1}{X} \frac{dC}{dX} = \alpha^2 \frac{C}{1 + \beta C} \tag{5}$$

at  $X = 0$  :  $\frac{dC}{dX} = 0$  (6)

at  $X = 1$  :  $C = 1$  (without external mass transfer resistance) (7)

which is the mathematical model expressing the dimensionless substrate concentration,  $C$  in the pellet [6]:

To describe the mass transfer limitation effect on the overall reaction rate, the overall effectiveness factor,  $\eta$  is given [14] by

$$\eta = \frac{\text{reaction rate}}{\text{reaction rate in the absence of internal and external resistances}} \tag{8}$$

Under steady state conditions, the reaction rate can be evaluated from the concentration profile obtained from the solution of equation (5) by the integration of the reaction rate from the pellet surface to the center and hence the effectiveness factor  $\eta$  is obtained by integrating the concentration profile for which the substrate concentration is taken in the bulk fluid phase, as given in equation (9) and also the effectiveness factor  $\eta$  is obtained by differentiating the concentration profile as given as follows:

$$\eta = \frac{g(1 + \beta)}{\alpha^2} \int_0^1 \frac{C}{1 + \beta C} X^{g-1} dX = \frac{g(1 + \beta)}{\alpha^2} \left( \frac{dC}{dX} \right)_{at X = 1} \tag{9}$$

### 3. AN ANALYTICAL EXPRESSION FOR THE SUBSTRATE CONCENTRATION ON IMMOBILIZED ENZYME REACTIONS USING TAYLOR’S SERIES METHOD

There are several analytical and numerical methods in our mathematical modeling field to deal with the nonlinear models and their solutions subject to the given initial and boundary conditions, such as Variational iteration method (VIM) [10, 15], the Taylor’s series method [13, 14, 16], Adomian decomposition method [17], Modified ADM [11, 17, 18], the Akbari-Ganji method [19], Homotopy perturbation method [20-25] and the finite difference methods, etc.

In this paper, the Taylor series method is applied to solve the nonlinear model (equations (5)-(7)) for the immobilized enzyme reactions as per our assumptions considered for our enzyme kinetics with respect to the three geometries viz. planar, cylindrical and spherical. Then the results are compared with the previous results of the same model solved by the respective authors using He’s Variational Iteration method and the Modified Adomian Decomposition method (MADM). Amongst these three methods, it is found that the Taylor’s series method yields the best approximations and it converges at its fourth order itself.

The analytical expression of the dimensionless substrate concentration on immobilized enzyme reaction, obtained by solving (5) using Taylor’s series method, has been derived in (Appendix A) and is obtained as

$$\begin{aligned}
 C(X) = & 1 + \frac{m(X-1)}{1!} + \frac{(X-1)^2}{2!} \left[ \frac{\alpha^2}{1+\beta} - (g-1)m \right] \\
 & + \frac{(X-1)^3}{3!} \left[ g(g-1)m - \frac{(g-1)\alpha^2}{1+\beta} + \frac{m\alpha^2}{(1+\beta)^2} \right] \\
 & + \frac{(X-1)^4}{4!} \left[ \frac{\alpha^4}{(1+\beta)^3} - \frac{2(g-1)m\alpha^2}{(1+\beta)^2} - \frac{2m^2\alpha^2\beta}{(1+\beta)^3} + \frac{(g^2-1)\alpha^2}{(1+\beta)} - g(g^2-1)m \right] \\
 & + \dots\dots\dots
 \end{aligned} \tag{10}$$

where  $m$  values are obtained by applying the condition (6) in the derivative of the expression (10), as given in Appendix A and substituting various possible values of the parameters  $\alpha$  and  $\beta$ , the  $m$  values have been collected as given in the Tables 1, 3 and 5 corresponding to the geometries planar, cylindrical and spherical by replacing the pellet shape factor values such that  $g = 1$ ,  $g = 2$  and  $g = 3$  respectively in the general quadratic expression in  $m$  so obtained and given below:

$$2\alpha^2\beta m^2 + [(g^3 + 3g^2 + 2g)(1+\beta)^3 + (2g+1)\alpha^2(1+\beta)]m - \alpha^4 - [g^2 + 3g + 2]\alpha^2(1+\beta)^2 = 0 \tag{11}$$

On applying the concentration expression (10) in (9), we obtain the effectiveness factor  $\eta$  as given below:

$$\eta = \frac{gm(1+\beta)}{\alpha^2} \tag{12}$$

#### 4. THE PREVIOUS APPROXIMATE ANALYTICAL RESULTS OF THE NONLINEAR SYSTEM OF EQUATIONS

4.1. *The previous analytical results using Variational Iteration Method (Saibavani and Senthamarai [10])*

Saibavani and Senthamarai [10], derived the analytical expression for the dimensionless concentration profile by solving the nonlinear equation (5) with the boundary conditions (6) and (7) by He’s Variational iteration method. The approximate analytical expression so obtained for the concentration profile by the Variational Iteration method is given below.

$$C(x) = l + \frac{x^2}{2(1-g)} [2(1-l) - \alpha^2 l + \alpha^2 \beta l^2] + \frac{x^4}{4(1-g)} [2\alpha^2 \beta l(1-l) - (1-l)\alpha^2] + \frac{x^6}{6(1-g)} [\alpha^2 \beta (1-l)^2] \tag{13}$$

where  $l = \frac{-(2\alpha^2 \beta - 3\alpha^2 - 12g) - \sqrt{-(2\alpha^2 \beta - 3\alpha^2 - 12g)^2 - 8\alpha^2 \beta (2\alpha^2 \beta - 3\alpha^2 + 12g)}}{4\alpha^2 \beta}$  \tag{14}

The analytical expression (13) fails to imply the results for the planar geometry, as it is invalid for the planar pellet shape factor value  $g = 1$ . But the Taylor’s series method as well as the MADM imply the analytical results for all the three geometries viz. planar, cylindrical and spherical geometries and so hereby only the TSM and MADM results are compared with the numerical results for the case of planar geometry as produced in Table 2(a) and Table 2(b). The effectiveness factor  $\eta$  for the concentration given under VIM has been found using (13) in (9), as

$$\eta = g(1+\beta) \left( \frac{l + \frac{[2(1-l) - \alpha^2 l + \alpha^2 \beta l^2]}{2(g+2)(1-g)}}{g} + \frac{[2\alpha^2 \beta l(1-l) - (1-l)\alpha^2]}{4(g+4)(1-g)} + \frac{[\alpha^2 \beta (1-l)^2]}{6(g+6)(1-g)} \right) \tag{15}$$

The dimensionless substrate concentration for planar geometry and higher values of the parameters for other geometries has not been found by this method since it is not supported for them.

4.2. *The previous analytical results using Modified Adomian Decomposition Method (Krishnan Lakshmi Narayanan et al. [11])*

Krishnan Lakshmi Narayanan et al. [11], derived the analytical expression for the dimensionless concentration profile by solving the nonlinear equation (5) by Modified Adomian Decomposition method. The approximate analytical expression so obtained for the concentration profile by the MADM is given below.

$$C(X) = 1 + \frac{1}{2g} \left[ \frac{\alpha^2}{(1+\beta)} (X^2 - 1) + \frac{\alpha^4}{60(1+\beta)^3} (3X^4 - 10X^2 + 7) \right] \tag{16}$$

The given geometry wise effectiveness factor values are obtained based on the solution expression (15) as follows: The general expression for the effectiveness factor has been derived using (15) in (9), as

$$\eta = 1 - \frac{\phi^2}{15(1 + \beta)^2} \tag{17}$$

and this expression is common for all three geometries since the expression is independent of  $g$  and it gives accurate results only for elliptical geometry. From the Tables (7)-(9), we can vcinfer that the numerical results are closed to the analytical results obtained by this method only for elliptical geometry.

### 5. IFLUENCE OF GEOMETRY

#### 5.1 PLANAR GEOMETRY

When  $g = 1$ , the equation (10) yields the concentration of the substrate  $C$  in the case of planar shape pellet, such a

$$C(X) = 1 + \frac{m(X - 1)}{1!} + \frac{(X - 1)^2}{2!} \left[ \frac{\alpha^2}{1 + \beta} \right] + \frac{(X - 1)^3}{3!} \left[ \frac{m\alpha^2}{(1 + \beta)^2} \right] + \frac{(X - 1)^4}{4!} \left[ \frac{\alpha^4}{(1 + \beta)^3} - \frac{2m^2\alpha^2\beta}{(1 + \beta)^3} \right] + \dots \tag{18}$$

where  $m$  is obtained by applying the condition (6) as follows:

By applying the condition (6) in the equation (18), we have

$$2\alpha^2\beta m^2 + [6(1 + \beta)^3 + 3\alpha^2(1 + \beta)]m - \alpha^4 - 6\alpha^2(1 + \beta)^2 = 0 \tag{19}$$

The numerical values of ‘ $m$ ’ for various possible values of the parameters  $\alpha$  and  $\beta$  satisfying the above equation (19) for the planar geometry are given in Table 1 which is used to plot the Figure 2 and to prepare the Table 2(a) and Table 2(b).

**Table 1.** Numerical values of the parameter  $m$  for various values of the parameters  $\alpha$  and  $\beta$  in the case of planar shape pellet.

$\alpha \backslash \beta$	0.1	0.25	0.5	0.75	1	5	10
0.01	0.009869	0.060654	0.229470	0.476364	0.771700	9.001416	28.914800
0.1	0.009066	0.055860	0.212830	0.444807	0.722630	6.545500	16.202000
0.5	0.006660	0.041281	0.160500	0.344295	0.572600	4.094000	8.558800
1	0.005000	0.031086	0.122300	0.267367	0.455300	3.351100	6.418900
10	0.000910	0.005681	0.022710	0.051054	0.090640	1.921370	4.197100
100	0.000100	0.000619	0.002480	0.005569	0.009900	0.247270	0.983800
500	0.000020	0.000125	0.000500	0.001123	0.001996	0.049900	0.199570
1000	0.000010	0.000062	0.000250	0.000562	0.000999	0.024970	0.099900

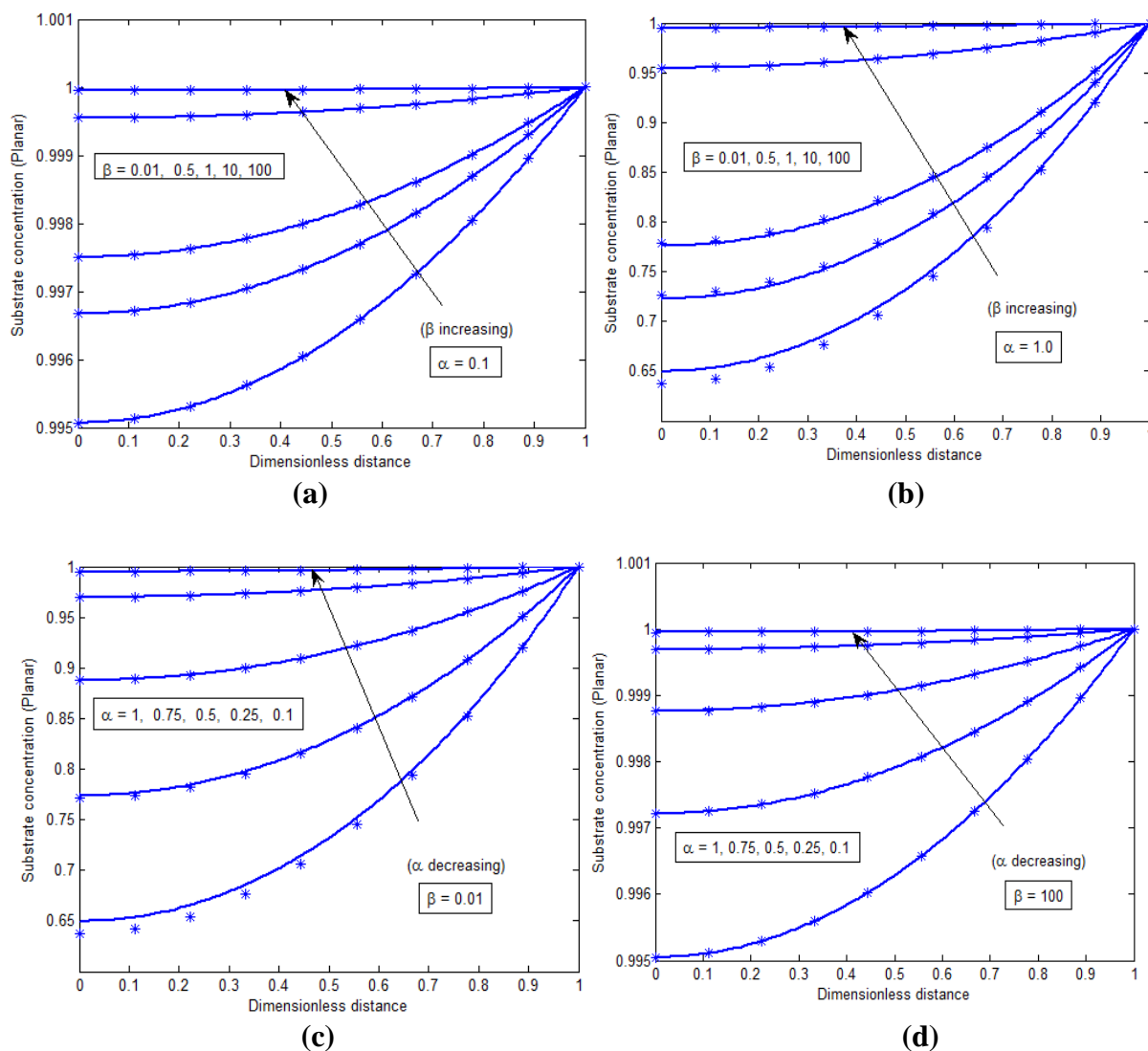


**Figure 2.** The dimensionless substrate concentration  $C(X)$  versus the dimensionless distance  $X$  for the different values of the parameters  $\alpha$  and  $\beta$  under the planar geometry, where the blue solid line represents the numerical results and (\*) represents the analytical results using Eq. (18). **(a)** Concentration variations while fixing that  $\alpha = 0.1$  and varying the  $\beta$  values. **(b)** Concentration variations while fixing that  $\alpha = 1.0$  and varying the  $\beta$  values. **(c)** Concentration variations while fixing that  $\beta = 0.01$  and varying the  $\alpha$  values. **(d)** Concentration variations while fixing that  $\beta = 100$  and varying the  $\alpha$  values.

Moreover, using (12), the effectiveness factor  $\eta$  under this geometry is obtained as

$$\eta = \frac{(1 + \beta)}{\alpha^2} m \tag{20}$$

The nonlinear reaction-diffusion equation (5) of our model along with the boundary conditions (6) and (7) has been solved for the dimensionless substrate concentration  $C(X)$  by the Taylor’s series method, assuming that  $C'(1)=m$ , a positive constant. The dimensionless substrate concentration so

obtained has been given by the equation (10) and the values of  $m$  have been generated by applying the boundary condition (6) in (A.11) and resulted as (A.12). If the pellet shape factor,  $g = 1$ , then the equation (10) implies the dimensionless concentration profile with respect to a planar geometrical pellet as given by the equation (18) and its corresponding  $m$  values have been calculated from (A.12) and tabulated as Table 1. Here, for various values of the dimensionless parameters  $\alpha$  and  $\beta$ , the dimensionless concentration profile has been prepared and clearly observed that the concentration levels obtained from both the analytical solution as well as the numerical solution have synchronized with each other for various values of the parameters, as resulted in the Figures. 2.(a)-2.(d), of which the Figures. 2.(a) and 2.(b) show that the dimensionless substrate concentration level increases in accordance with the increasing of  $\beta$  values while  $\alpha$  being fixed at the least value 0.1 or at the highest value 1 of its considerable range, on the other hand, Figures. 2.(c) and 2.(d) show that the concentration level increases in accordance with the decreasing of  $\alpha$  values while  $\beta$  being fixed at the least value 0.01 or at the highest value 100 of its considerable range. Moreover, here the dimensionless concentration profile has also been prepared using MADM [11] and the comparison table has been prepared for showing the variations between the concentration levels for such sets of values of the parameters  $\alpha$  and  $\beta$  for both the analytical solutions, as produced in Table 2. From this comparison, it is clearly observed that concentration levels under the TSM results are quite better than that of MADM for smaller values of the parameters  $\alpha$  and  $\beta$  and that the MADM results are quite better than that of TSM for higher values of the parameters  $\alpha$  and  $\beta$ , but they are at the same levels when rounding off the results upto 2 decimal places. As the VIM [10] fails to apply for this geometry, it is not taken for comparison here. The overall effectiveness factor,  $\eta$  corresponding to this geometry has been given in the equation (20) and the values obtained from which for the average rate have been tabulated as Table 7. Figure. 3(a) shows the flow of the effectiveness factor  $\eta$  against the Thiele modulus  $\alpha$  and Figure. 3(b) shows the flow of the effectiveness factor  $\eta$  against the Michaelis-Menten constant  $\beta$ , under this geometry. An increasing value of the Thiele modulus increases the effectiveness factor, while the higher values of the Michaelis-Menten constant decreases the effectiveness factor.

**Table 2(a).** Comparison of the normalized steady state substrate concentration values of the TSM and the MADM [11] with the numerical solution, for various values of the parameters  $\alpha, \beta$  and the corresponding values of  $m$ , with respect to Planar pellet.

$X$	Concentration $C(X)$									
	$\alpha = 0.1, \beta = 0.01$ and $m = 0.009869$					$\alpha = 0.5, \beta = 0.5$ and $m = 0.1605$				
	Numerical	TSM	MADM	Error in TSM	Error in MADM	Numerical	TSM	MADM	Error in TSM	Error in MADM
0	0.995100	0.995100	0.995055	0	0.004505	0.920500	0.920600	0.917747	0.010864	0.299086
0.1	0.995149	0.995100	0.995105	0.004884	0.004463	0.921231	0.921300	0.918565	0.007440	0.289410
0.2	0.995295	0.995300	0.995253	0.000482	0.004233	0.923565	0.923700	0.921019	0.014604	0.275643
0.3	0.995540	0.995500	0.995500	0.003998	0.004018	0.927501	0.927600	0.925112	0.010676	0.257598
0.4	0.995882	0.995900	0.995846	0.001767	0.003613	0.933039	0.933100	0.930845	0.006533	0.235126
0.5	0.996323	0.996300	0.996290	0.002308	0.003220	0.940179	0.940300	0.938223	0.012838	0.208005
0.6	0.996862	0.996800	0.996835	0.006179	0.002734	0.948922	0.949000	0.947251	0.008245	0.176057

0.7	0.997498	0.997500	0.997478	0.000180	0.002052	0.959266	0.959300	0.957935	0.003501	0.138728
0.8	0.998233	0.998200	0.998219	0.003286	0.001372	0.971213	0.971200	0.970282	0.001367	0.095837
0.9	0.999065	0.999100	0.999060	0.003463	0.000490	0.984762	0.984800	0.984301	0.003824	0.046848
1	0.999996	1	1	0.000400	0.000400	0.999914	1	1	0.008641	0.008601
<b>Average Error</b>				0.002450	0.002827	<b>Average Error</b>			0.008049	0.184631

**Table 2(b).** Comparison of the normalized steady state substrate concentration values of the TSM and the MADM [11] with the numerical solution, for various values of the parameters  $\alpha, \beta$  and the corresponding values of  $m$ , with respect to Planar pellet.

X	Concentration $C(X)$									
	$\alpha = 1, \beta = 0.01$ and $m = 0.7717$					$\alpha = 2, \beta = 5$ and $m = 0.63161$				
	Numerical	TSM	MADM	Error in TSM	Error in MADM	Numerical	TSM	MADM	Error in TSM	Error in MADM
0	0.650000	0.637227	0.5615683	1.965126	13.60488	0.690000	0.690035	0.6709877	0.005087	2.755412
0.1	0.653776	0.640764	0.5657124	1.990360	13.47001	0.693109	0.693030	0.6742594	0.011387	2.719509
0.2	0.663688	0.651285	0.5781738	1.868810	12.88471	0.702269	0.702060	0.684077	0.029716	2.590427
0.3	0.680072	0.668732	0.5990398	1.667428	11.91523	0.717532	0.717196	0.7004471	0.046796	2.381091
0.4	0.703264	0.693143	0.6284562	1.439177	10.63724	0.738950	0.738509	0.7233807	0.059784	2.106996
0.5	0.733600	0.724650	0.6666265	1.220072	9.129424	0.766575	0.766067	0.7528935	0.066296	1.784754
0.6	0.771416	0.763482	0.7138131	1.028549	7.467166	0.800458	0.799941	0.7890054	0.064542	1.430702
0.7	0.817048	0.809964	0.770336	0.867036	5.717161	0.840650	0.840201	0.8317409	0.053356	1.059760
0.8	0.870832	0.864517	0.836574	0.725139	3.933942	0.887203	0.886918	0.8811289	0.032171	0.684658
0.9	0.933104	0.927658	0.9129636	0.583600	2.158428	0.940169	0.940161	0.9372027	0.000932	0.315554
1	1.004200	1	1	0.418243	0.418243	0.999600	1	1	0.040016	0.040016
<b>Average Error</b>				1.252140	8.303312	<b>Average Error</b>			0.037280	1.624444

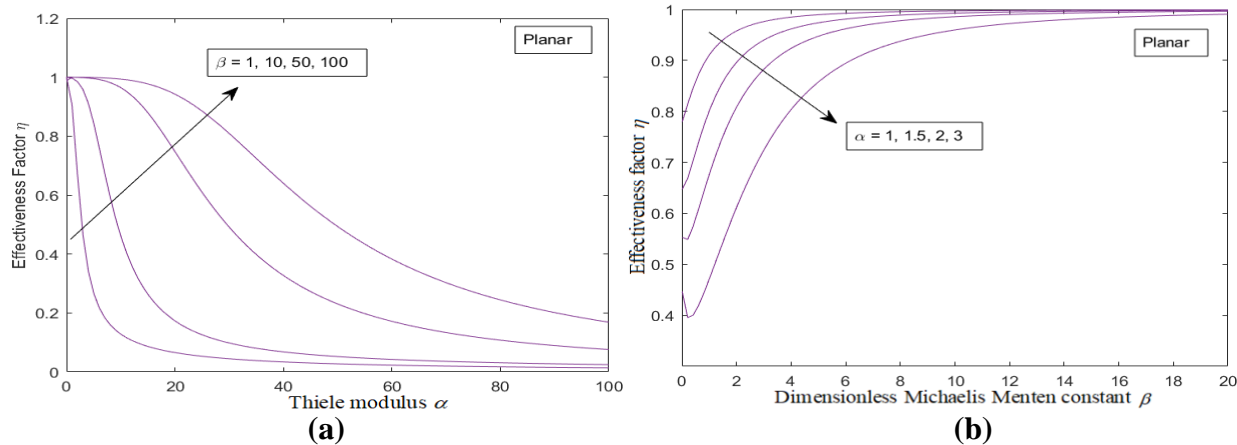


**Figure 3.** (a) The Effectiveness factor  $\eta$  against Thiele modulus  $\alpha$ . (b) The effectiveness factor  $\eta$  against the dimensionless Michaelis-Menten constant  $\beta$ .

5.2 Cylindrical Geometry

When  $g = 2$ , the equation (10) yields the concentration of the substrate  $C$  in the case of cylindrical shape pellet, such as

$$C(X) = 1 + \frac{m(X-1)}{1!} + \frac{(X-1)^2}{2!} \left[ \frac{\alpha^2}{1+\beta} - m \right] + \frac{(X-1)^3}{3!} \left[ 2m - \frac{\alpha^2}{1+\beta} + \frac{m\alpha^2}{(1+\beta)^2} \right] + \frac{(X-1)^4}{4!} \left[ \frac{\alpha^4}{(1+\beta)^3} - \frac{2m\alpha^2}{(1+\beta)^2} - \frac{2m^2\alpha^2\beta}{(1+\beta)^3} + \frac{3\alpha^2}{(1+\beta)} - 6m \right] + \dots \tag{21}$$

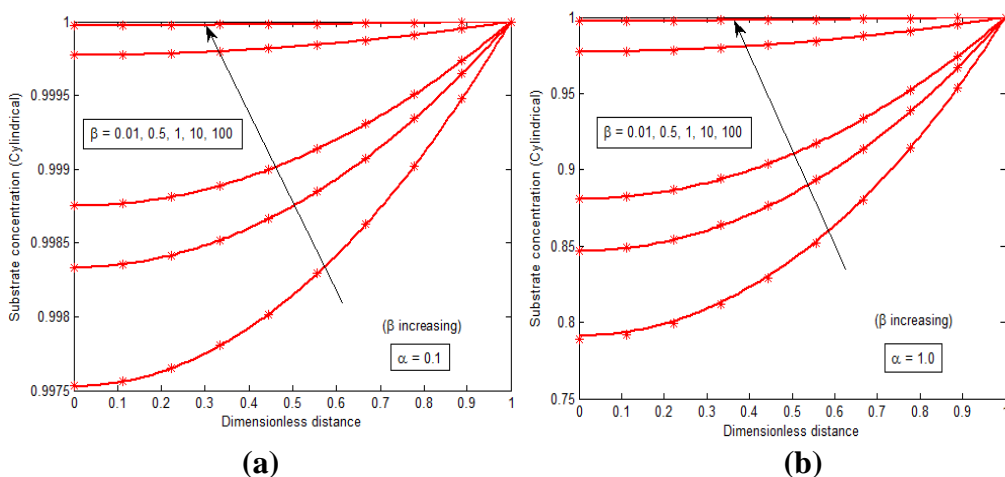
where  $m$  is obtained by applying the condition (6) as follows:

By applying the condition (6) using (21), we have

$$2\alpha^2\beta m^2 + [24(1+\beta)^3 + 5\alpha^2(1+\beta)]m - \alpha^4 - 12\alpha^2(1+\beta)^2 = 0 \tag{22}$$

**Table 3.** Numerical values of the parameter  $m$  for various values of the parameters  $\alpha$  and  $\beta$  in the case of cylindrical shape pellet.

$\alpha \backslash \beta$	0.1	0.25	0.5	0.75	1	5	10
0.01	0.004944	0.030707	0.120152	0.261222	0.444543	6.045647	19.720234
0.1	0.004541	0.028227	0.110804	0.241948	0.413572	5.071792	13.456074
0.5	0.003332	0.020761	0.082182	0.181713	0.315261	3.620934	7.855996
1	0.002499	0.015594	0.062008	0.138115	0.241994	3.065746	6.123867
10	0.000455	0.002841	0.011361	0.025553	0.045406	1.090385	3.493117
100	0.000050	0.000309	0.001238	0.002785	0.004950	0.123721	0.494247
500	0.000010	0.000062	0.000250	0.000561	0.000998	0.024950	0.099795
1000	0.000005	0.000031	0.000125	0.000281	0.000500	0.012488	0.049949



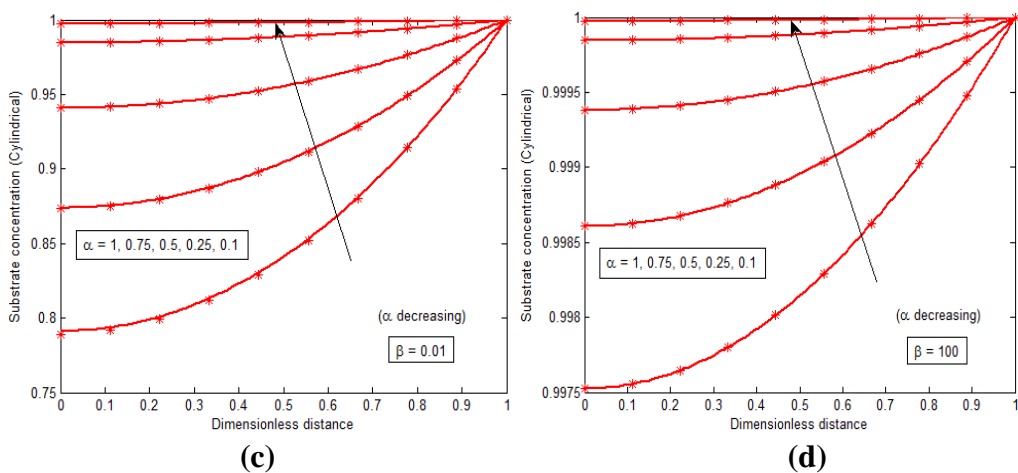


**Figure 4.** The dimensionless substrate concentration  $C(X)$  versus the dimensionless distance  $X$  for the different values of the parameters  $\alpha$  and  $\beta$  under the cylindrical geometry, where the red solid line represents the numerical results and (\*) represents the analytical results using Eq. (21). **(a)** Concentration variations while fixing that  $\alpha = 0.1$  and varying the  $\beta$  values. **(b)** Concentration variations while fixing that  $\alpha = 1.0$  and varying the  $\beta$  values. **(c)** Concentration variations while fixing that  $\beta = 0.01$  and varying the  $\alpha$  values. **(d)** Concentration variations while fixing that  $\beta = 100$  and varying the  $\alpha$  values.

The numerical values of ‘ $m$ ’ for various possible values of the parameters  $\alpha$  and  $\beta$ , satisfying the above equation (22) for the cylindrical geometry are given in Table 3, which is used to plot the Figure 4 and to prepare the Table 4(a) and Table 4(b).

And then using (12), the effectiveness factor  $\eta$  under this geometry is obtained as

$$\eta = \frac{2(1 + \beta)}{\alpha^2} m \tag{23}$$

If the pellet shape factor,  $g = 2$ , then the equation (10) implies the dimensionless concentration profile with respect to a cylindrical geometrical pellet as given by the equation (21) and its corresponding  $m$  values have been calculated from (A.12) and tabulated as Table 3. Here, for various values of the dimensionless parameters  $\alpha$  and  $\beta$ , the dimensionless concentration profile based on TSM solution has been prepared and clearly observed that the concentration levels obtained from both the analytical solution as well as the numerical solution have synchronized with each other, while applying TSM analytical solution which converges at its fourth order itself, as resulted in the Figures. 4.(a) - 4.(d), of which the Figures. 4.(a) and 4.(b) show that the dimensionless substrate concentration level increases in accordance with the increasing of  $\beta$  values while  $\alpha$  being fixed at the least value 0.1 or at the highest value 1 of its considerable range, on the other hand, Figures. 4.(c) and 4.(d) show that the concentration level increases in accordance with the decreasing of  $\alpha$  values while  $\beta$  being fixed at the least value 0.01 or at the highest value 100 of its considerable range. Moreover, here the VIM [10] of analytical results have also been obtained and compared with the numerical results, where it is found that VIM fails to give results for the higher values of the parameter  $\alpha$  and for  $\beta > 1$ , but

both the TSM and MADM methods yield the results for all the values of the parameters, confined to the given boundary conditions.

Here it is also found that VIM fails to give results for the higher values of the parameters  $\alpha$  and  $\beta$ . Accordingly, the comparison table has been prepared for showing the variations between the concentration levels for various values of the parameters  $\alpha$  and  $\beta$ , as in Table 4. From such a comparison, it is clearly observed that concentration levels under the TSM results are quite better than that of both the VIM [10] and the MADM [11] results for almost all the values of the parameters  $\alpha$  and  $\beta$  and that the MADM results are quite better than that of both the TSM and the VIM for higher values of the parameter  $\beta \geq 700$ , but as the maximum value applicable for  $\beta$  is nearly 700, put together it is inferred that the TSM gives best results comparing to the other two methods. Anyway the VIM [10] produces poor results while comparing to the TSM and MADM results. The overall effectiveness factor,  $\eta$  corresponding to this geometry has been given in the equation (23) and the values obtained from which for the average rate have been tabulated as Table 8(a) and Table 8(b). Further it is observed that the effectiveness factor  $\eta$  values here also constantly maintain a relationship with the dimensionless substrate concentration under the Michaelis kinetics ( $\beta$ ), such that  $\eta = 1 + \beta$ , for all  $\alpha$  of its considerable range as obtained in the Table 8(a) and Table 8(b). Figure. 5(a) shows that the effectiveness factor  $\eta$  maintains the above given relation with the  $\beta$  values throughout the Theile modulus  $\alpha$  values of its range and Figure. 5(b) shows that the flow of the effectiveness factor is independent of  $\alpha$  values and maintains the same above given relation with  $\beta$ , on varying the  $\beta$  values of its range under the cylindrical geometry.

**Table 4(a).** Comparison of the normalized steady state substrate concentration values under VIM [10], MADM [11] and the Taylor’s series method with the numerical solution for various values of the parameters  $\alpha, \beta$  and the corresponding values of  $m$  under cylindrical geometry.

X	Concentration C(X)													
	$\alpha = 0.1, \beta = 0.01$ and $m = 0.004944$						$\alpha = 0.5, \beta = 0.5$ and $m = 0.082182$							
	Numerical	TSM	MADM	VIM	Error in TSM	Error in MADM	Error in VIM	Numerical	TSM	MADM	VIM	Error in TSM	Error in MADM	Error in VIM
0	0.997500	0.997500	0.997528	0.997528	0	0.002765	0.002807	0.959200	0.959200	0.958873	0.968760	0	0.034043	0.996664
0.1	0.997525	0.997600	0.997552	0.997553	0.007560	0.002736	0.002807	0.959584	0.959600	0.959282	0.969072	0.001690	0.031427	0.988762
0.2	0.997599	0.997600	0.997626	0.997627	0.000140	0.002750	0.002807	0.960788	0.960800	0.960510	0.970008	0.001270	0.028973	0.959629
0.3	0.997722	0.997800	0.997750	0.997750	0.007810	0.002807	0.002806	0.962812	0.962800	0.962556	0.971569	0.001249	0.026600	0.909523
0.4	0.997895	0.997900	0.997923	0.997923	0.000500	0.002807	0.002806	0.965656	0.965700	0.965423	0.973754	0.004510	0.024171	0.838601
0.5	0.998117	0.998100	0.998145	0.998145	0.001734	0.002851	0.002805	0.969321	0.969300	0.969112	0.976563	0.002172	0.021593	0.747121
0.6	0.998389	0.998400	0.998417	0.998417	0.001090	0.002842	0.002805	0.973806	0.973800	0.973626	0.979999	0.000602	0.018517	0.635958
0.7	0.998710	0.998700	0.998739	0.998738	0.001033	0.002880	0.002804	0.979111	0.979100	0.978968	0.984060	0.001110	0.014644	0.505459
0.8	0.999081	0.999100	0.999110	0.999109	0.001900	0.002868	0.002803	0.985236	0.985200	0.985141	0.988747	0.003662	0.009631	0.356361
0.9	0.999501	0.999500	0.999530	0.999529	0.000108	0.002907	0.002801	0.992181	0.992200	0.992150	0.994061	0.001870	0.003091	0.189482
1	0.999971	1	1	1	0.002940	0.002900	0.002900	0.999947	1	1	1	0.005290	0.005300	0.005300
	<b>Average Error</b>				0.002256	0.002828	0.002814	<b>Average Error</b>				0.002130	0.019817	0.648442

**Table 4 (b).** Comparison of the normalized steady state substrate concentration values under VIM [10], MADM [11] and the Taylor’s series method with the numerical solution for various values of the parameters  $\alpha, \beta$  and the corresponding values of  $m$  under cylindrical geometry.

X	Concentration C(X)					Concentration C(X)				
	$\alpha = 1, \beta = 0.01$ and $m = 0.444543$					$\alpha = 2, \beta = 5$ and $m = 0.327997$				
	Numerical	TSM	MADM	Error in TSM	Error in MADM	Numerical	TSM	MADM	Error in TSM	Error in MADM
0	0.790000	0.789033	0.780784	0.122454	1.166566	0.840000	0.837596	0.835494	0.286193	0.536449
0.1	0.792215	0.791073	0.782856	0.144111	1.181349	0.841659	0.839196	0.837130	0.292653	0.538125
0.2	0.798180	0.797173	0.789087	0.126187	1.139232	0.846535	0.844004	0.842039	0.298984	0.531187
0.3	0.808045	0.807323	0.799520	0.088818	1.055026	0.854646	0.852036	0.850224	0.305452	0.517495
0.4	0.821960	0.821573	0.814228	0.047088	0.940669	0.866010	0.863306	0.861690	0.312157	0.498751
0.5	0.840075	0.839986	0.833313	0.010635	0.804896	0.880643	0.877833	0.876447	0.319041	0.476441
0.6	0.862540	0.862681	0.856907	0.016366	0.653124	0.898562	0.89563	0.894503	0.325893	0.451798
0.7	0.889505	0.889815	0.885168	0.034857	0.487572	0.919787	0.916730	0.915871	0.332376	0.425777
0.8	0.921120	0.921583	0.918287	0.050233	0.307562	0.944333	0.941141	0.940564	0.338046	0.399050
0.9	0.957535	0.958219	0.956482	0.071469	0.109990	0.972218	0.968889	0.968601	0.342381	0.372013
1	0.998900	1	1	0.110121	0.110121	1.003460	1	1	0.344807	0.344807
	<b>Average Error</b>			0.07475	0.723282	<b>Average Error</b>			0.317999	0.462899

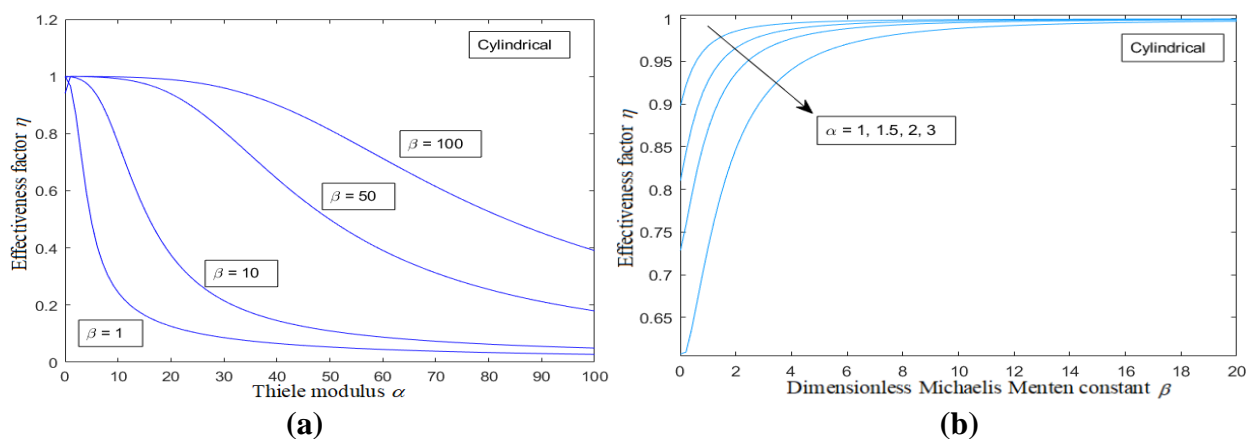


**Figure 5. (a)** The effectiveness factor  $\eta$  against Thiele modulus  $\alpha$ . **(b)** The effectiveness factor  $\eta$  against the dimensionless Michaelis-Menten constant  $\beta$ .

### 5.3 Spherical Geometry

When  $g = 3$ , the equation (10) yields the concentration of the substrate  $C$  in the case of spherical shape pellet, such as

$$\begin{aligned}
 C(X) = & 1 + \frac{m(X-1)}{1!} + \frac{(X-1)^2}{2!} \left[ \frac{\alpha^2}{1+\beta} - 2m \right] + \frac{(X-1)^3}{3!} \left[ 6m - \frac{2\alpha^2}{1+\beta} + \frac{m\alpha^2}{(1+\beta)^2} \right] \\
 & + \frac{(X-1)^4}{4!} \left[ \frac{\alpha^4}{(1+\beta)^3} - \frac{4m\alpha^2}{(1+\beta)^2} - \frac{2m^2\alpha^2\beta}{(1+\beta)^3} + \frac{8\alpha^2}{(1+\beta)} - 24m \right] + \dots
 \end{aligned}
 \tag{24}$$

where  $m$  is obtained by applying the condition (6) as follows:

By applying the condition (6) using (24), we have

$$2\alpha^2\beta m^2 + [60(1+\beta)^3 + 7\alpha^2(1+\beta)]m - \alpha^4 - 20\alpha^2(1+\beta)^2 = 0 \tag{25}$$

The numerical values of ‘ $m$ ’ for various possible values of the parameters  $\alpha$  and  $\beta$ , satisfying the above equation (25) for the spherical geometry are given in Table 5, which is used to plot the Figure 6 and to prepare the Table 6(a) and Table 6(b).

**Table 5.** Numerical values of the parameter  $m$  for various values of the parameters  $\alpha$  and  $\beta$  in the case of spherical shape pellet.

$\alpha \backslash \beta$	0.1	0.25	0.5	0.75	1	5	10
0.01	0.003298	0.020543	0.081197	0.179226	0.310650	4.711243	15.069882
0.1	0.003029	0.018875	0.074735	0.165407	0.287614	4.193281	11.501229
0.5	0.002222	0.013863	0.055146	0.122935	0.215744	3.209596	7.310227
1	0.001666	0.010406	0.041493	0.092865	0.163859	2.717713	5.887256
10	0.000303	0.001894	0.007575	0.017040	0.030286	0.744002	2.710246
100	0.000033	0.000206	0.000825	0.001856	0.003300	0.082494	0.329782
500	0.000007	0.000042	0.000166	0.000374	0.000665	0.016633	0.066532
1000	0.000003	0.000021	0.000083	0.000187	0.000333	0.008325	0.033300

Applying again (12), the effectiveness factor  $\eta$  under the spherical geometry is obtained as

$$\eta = \frac{3(1+\beta)}{\alpha^2} m \tag{26}$$

If the pellet shape factor,  $g = 3$ , then the equation (10) implies the dimensionless concentration profile with respect to a spherical geometrical pellet as given by the equation (24) and its corresponding  $m$  values have been calculated from (A.12) and tabulated as Table 5. Here, for various values of the dimensionless parameters  $\alpha$  and  $\beta$ , the dimensionless concentration profile of TSM solution has been prepared and clearly observed that the concentration levels obtained from both the analytical solution as well as the numerical solution have synchronized with each other, while applying TSM of analytical solutions which converge at its fourth order itself, as resulted in the Figures. 6.(a)-6.(d), of which the Figures. 6.(a) and 6.(b) show that the dimensionless substrate concentration level increases in accordance with the increasing of  $\beta$  values while  $\alpha$  being fixed at the least value 0.1 to at the highest value 1 of its considerable range, on the other hand, Figures. 6.(c) and 6.(d) show that the concentration level increases in accordance with the decreasing of  $\alpha$  values while  $\beta$  being fixed at the least value 0.01 to the highest value 100 of its considerable range. Moreover, on comparison with the previous results obtained from both the MADM [11] and VIM [10] solutions, here it is observed that the TSM gives better results only for the values of the parameters  $\alpha$  and  $\beta < 0.5$  and that the MADM gives better results for the range of the parameters,  $\alpha$  and  $\beta \geq 0.5$ . Here it is also found that VIM fails to give results for the higher values of the parameters  $\alpha$  and  $\beta$ . Accordingly, the comparison table has been prepared for showing the variations between the concentration levels based on these three

methods for various values of the parameters  $\alpha$  and  $\beta$ , as in Table 6. The overall effectiveness factor,  $\eta$  corresponding to this geometry has been given in (26) and the values obtained from which for the average rate have been tabulated as in Table 9(a) and Table 9(b). Further it is observed that the effectiveness factor  $\eta$  values here also constantly maintain a relationship with the dimensionless substrate concentration under the Michaelis kinetics ( $\beta$ ), such that  $\eta = 1 + \beta$ , for all  $\alpha$  of its considerable range as obtained in the Table 9(a) and Table 9(b). Fig. 7(a) shows that the effectiveness factor  $\eta$  maintains the above given relation with the  $\beta$  values throughout the Thiele modulus  $\alpha$  values of its range and Figure 7(b) shows that the flow of the effectiveness factor is independent of  $\alpha$  values and maintains the same above given relation with  $\beta$ , on varying the  $\beta$  values of its range under the spherical geometry. The effectiveness factor rises as the Thiele modulus increases in value. Increasing the value of the Michaelis-Menten constant, on the other hand, reduces the effectiveness factor.

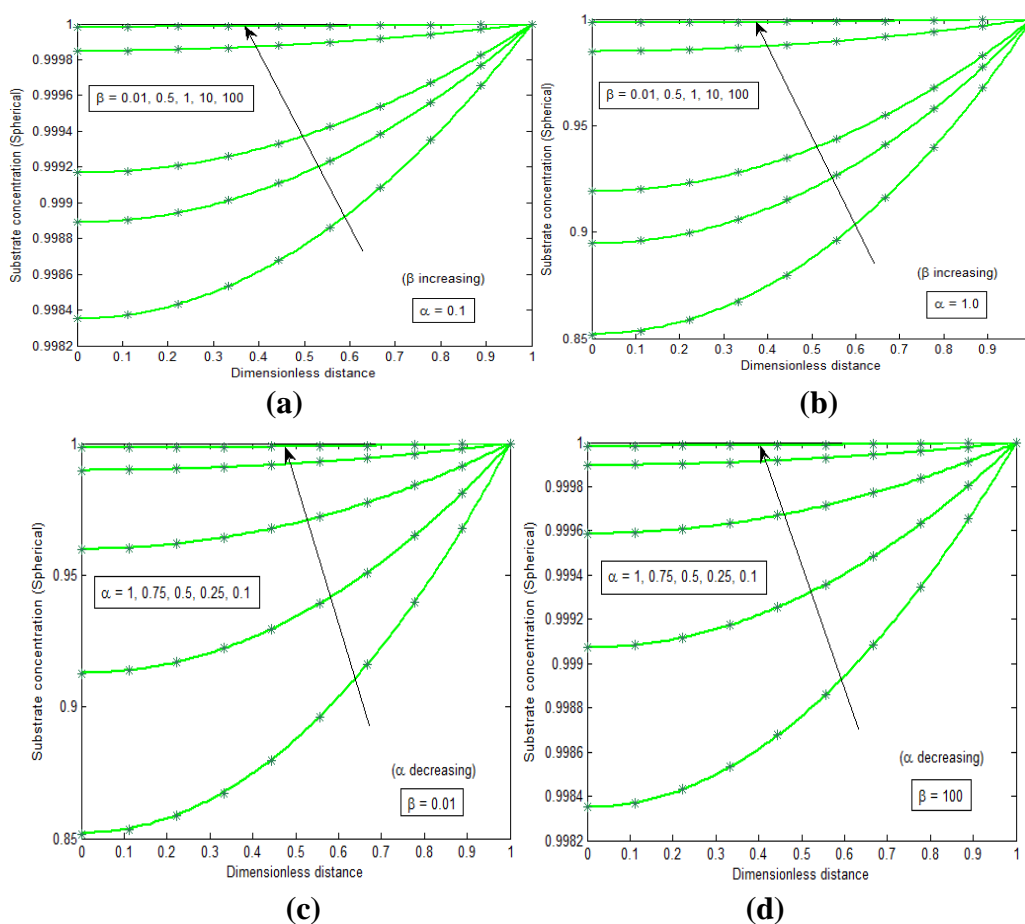


**Figure 6.** The dimensionless substrate concentration  $C(X)$  versus the dimensionless distance  $X$  for the different values of the parameters  $\alpha$  and  $\beta$  under the spherical geometry, where the green solid line represents the numerical results and (\*) represents the analytical results using Eq. (24). (a) Concentration variations while fixing that  $\alpha = 0.1$  and varying the  $\beta$  values. (b) Concentration variations while fixing that  $\alpha = 1.0$  and varying the  $\beta$  values. (c) Concentration variations while fixing that  $\beta = 0.01$  and varying the  $\alpha$  values. (d) Concentration variations while fixing that  $\beta = 100$  and varying the  $\alpha$  values.

**Table6 (a).** Comparison of the normalized steady state substrate concentration values under VIM [10], MADM [11] and the Taylor’s series method with the numerical solution for various values of the parameters  $\alpha, \beta$  and the corresponding values of  $m$  under spherical geometry.

X	Concentration $C(X)$													
	$\alpha = 0.1, \beta = 0.01$ and $m = 0.003298$						$\alpha = 0.5, \beta = 0.5$ and $m = 0.0551456$							
	Numerical	TSM	MADM	VIM	Error in TSM	Error in MADM	Error in VIM	Numerical	TSM	MADM	VIM	Error in TSM	Error in MADM	Error in VIM
0	0.998400	0.998400	0.998352	0.998351	0	0.004836	0.004908	0.972600	0.972600	0.972582	0.979170	0	0.001819	0.675509
0.1	0.998416	0.998400	0.998368	0.998368	0.001644	0.004788	0.004808	0.972861	0.972900	0.972855	0.979378	0.003983	0.000621	0.669880
0.2	0.998466	0.998400	0.998418	0.998417	0.006591	0.004845	0.004908	0.973673	0.973700	0.973673	0.980003	0.002763	0.000009	0.650116
0.3	0.998548	0.998500	0.998500	0.998500	0.004826	0.004807	0.004807	0.975036	0.975000	0.975037	0.981044	0.003650	0.000129	0.616182
0.4	0.998664	0.998600	0.998615	0.998615	0.006363	0.004873	0.004907	0.976949	0.976900	0.976948	0.982501	0.004970	0.000061	0.568300
0.5	0.998812	0.998800	0.998766	0.998763	0.001190	0.004842	0.004906	0.979412	0.979400	0.979408	0.984376	0.001250	0.000430	0.506835
0.6	0.998993	0.998900	0.998945	0.998944	0.009329	0.004813	0.004905	0.982427	0.982400	0.982417	0.986667	0.002700	0.001006	0.431584
0.7	0.999207	0.999200	0.999159	0.999159	0.000750	0.004786	0.004804	0.985991	0.986000	0.985978	0.989375	0.000877	0.001277	0.343208
0.8	0.999455	0.999400	0.999406	0.999406	0.005480	0.004859	0.004903	0.990107	0.990100	0.990094	0.992500	0.000690	0.001306	0.241691
0.9	0.999735	0.999700	0.999687	0.999686	0.003504	0.004831	0.004901	0.994773	0.994800	0.994767	0.996041	0.002729	0.000614	0.127466
1	1.000048	1	1	1	0.004826	0.004800	0.004800	0.999990	1	1	1	0.001050	0.001000	0.001000
	<b>Average Error</b>				0.004046	0.004825	0.00486	<b>Average Error</b>				0.002242	0.000752	0.439252

**Table 6 (b).** Comparison of the normalized steady state substrate concentration values under VIM [10], MADM [11] and the Taylor’s series method with the numerical solution for various values of the parameters  $\alpha, \beta$  and the corresponding values of  $m$  under spherical geometry.

X	Concentration $C(X)$									
	$\alpha = 1, \beta = 0.01$ and $m = 0.31065$					$\alpha = 2, \beta = 5$ and $m = 0.220449$				
	Numerical	TSM	MADM	Error in TSM	Error in MADM	Numerical	TSM	MADM	Error in TSM	Error in MADM
0	0.850000	0.851369	0.853856	0.161066	0.453657	0.890000	0.890528	0.890329	0.059375	0.036991
0.1	0.851524	0.852808	0.855237	0.150763	0.436095	0.891121	0.891613	0.891420	0.055139	0.033488
0.2	0.855732	0.857116	0.859391	0.161754	0.427617	0.894451	0.894869	0.894692	0.046738	0.026960
0.3	0.862708	0.864299	0.866347	0.184425	0.421766	0.899998	0.900304	0.900149	0.033974	0.016804
0.4	0.872536	0.874383	0.876152	0.211658	0.414430	0.907770	0.907922	0.907794	0.016823	0.002642
0.5	0.885300	0.887415	0.888876	0.238943	0.403876	0.917775	0.917733	0.917631	0.004568	0.015671
0.6	0.901084	0.903466	0.904605	0.264382	0.390681	0.930022	0.929744	0.929669	0.029891	0.038055
0.7	0.919972	0.922627	0.923445	0.288568	0.377549	0.944520	0.943966	0.943914	0.058696	0.064219
0.8	0.942048	0.945009	0.945525	0.314357	0.369053	0.961277	0.960408	0.960376	0.090407	0.093678
0.9	0.967396	0.970749	0.970988	0.346551	0.371293	0.980301	0.979082	0.979068	0.124342	0.125783
1	0.996100	1	1	0.391527	0.391527	1.001600	1	1	0.159744	0.159744
	<b>Average Error</b>			0.246727	0.405231	<b>Average Error</b>			0.061791	0.055821

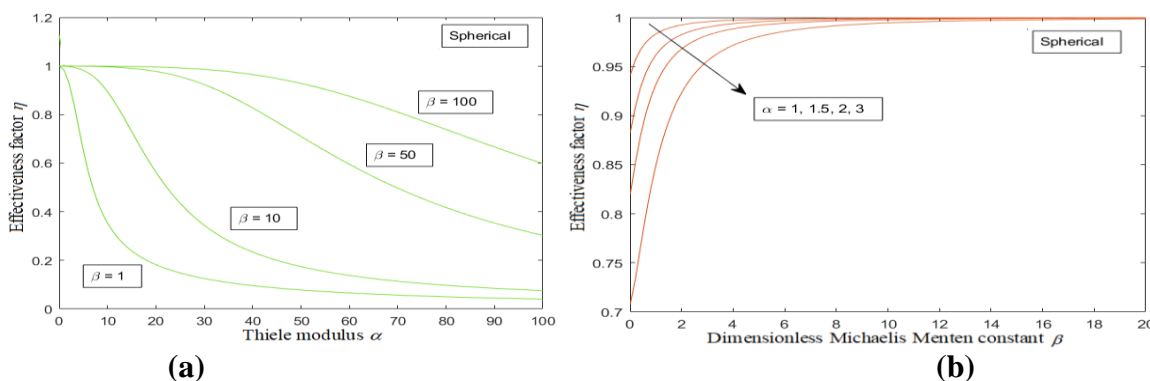


**Figure 7.** (a) The effectiveness factor  $\eta$  against Thiele modulus  $\alpha$ . (b) The effectiveness factor  $\eta$  against the dimensionless Michaelis-Menten constant  $\beta$

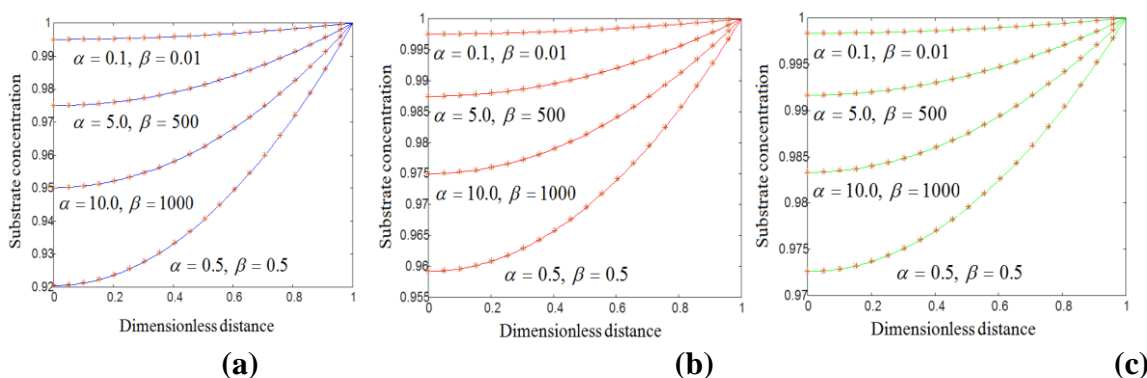


**Figure 8.** The dimensionless substrate concentration  $C(X)$  versus the dimensionless distance  $X$  for the different values of the parameters  $\alpha$  and  $\beta$ . (a) The concentration profile under the planar geometry, where the blue solid line (-) denotes the numerical results and (\*) denotes the analytical results using Eq. (18). (b) The concentration profile under the cylindrical geometry, where the red solid line (-) denotes the numerical results and (\*) denotes the analytical results using Eq. (21). (c) The concentration profile under the spherical geometry, where the green solid line (-) denotes the numerical results and (\*) denotes the analytical results using Eq. (24).

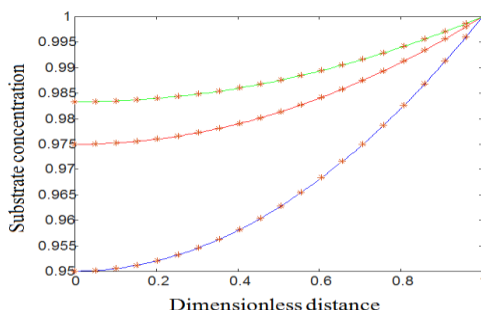


**Figure 9.** The comparison of the variations amongst the three geometrical outputs of the dimensionless substrate concentration  $C(X)$  versus the dimensionless distance  $X$  at a position for which the values of the parameters taken are  $\alpha = 10$  and  $\beta = 1000$ , in which the blue solid line with (\*) represents the solutions under planar geometry, the red solid line with (\*) represents the solutions under cylindrical geometry and the green solid line with (\*) represents the solutions under spherical geometry.

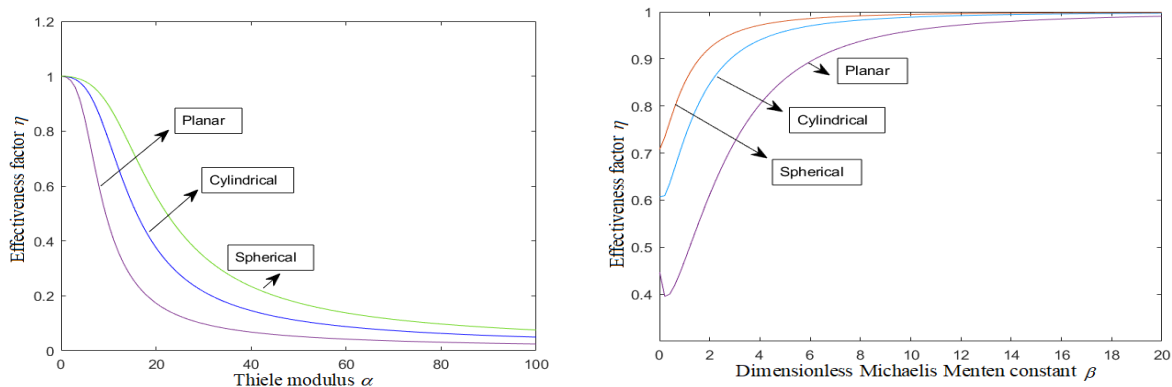


**Figure 10.** (a) The effectiveness factor  $\eta$  against Thiele modulus  $\alpha$ . (b) The effectiveness factor  $\eta$  against the dimensionless Michaelis-Menten constant  $\beta$ .

**Table 7.** The Comparison of the Effectiveness factor variations under TSM and MADM [11] analytical results with numerical results by planar shape pellet for various values of the Theile Modulus  $\alpha$  and various values of  $\beta$ .

$\beta$	$\alpha=1$						$\alpha=2$				$\alpha=3$				
	Numerical $\eta$	TSM $\eta$	MADM $\eta$	Error by TSM	Error by MADM	Numerical $\eta$	TSM $\eta$	MADM $\eta$	Error by TSM	Error by MADM	Numerical $\eta$	TSM $\eta$	MADM $\eta$	Error by TSM	Error by MADM
	$Ef$	$\eta$	$\eta$			$Ef$	$\eta$	$\eta$			$Ef$	$\eta$	$\eta$		
1	0.9088	0.9106	0.98333	0.1950	8.2013	0.6900	0.6762	0.93333	2.0036	35.2657	0.5002	0.4709	0.85000	5.8543	69.9245
10	0.9923	0.9970	0.99945	0.4788	0.7227	1.0003	0.9857	0.99780	1.4658	0.2543	0.9611	0.9597	0.99504	0.1481	3.5268
25	0.9884	0.9995	0.99990	1.1222	1.1636	1.0027	0.9977	0.99961	0.4953	0.3096	0.9866	0.9941	0.99911	0.7687	1.2725
50	0.9997	0.9999	0.99997	0.0153	0.0272	0.9949	0.9994	0.99990	0.4530	0.4983	0.9983	0.9986	0.99977	0.0303	0.1426
75	1.0032	0.9999	0.99999	0.3303	0.3246	0.9882	0.9998	0.99995	1.1714	1.1909	0.9969	0.9994	0.99990	0.2530	0.3011
100	1.0100	1.0000	0.99999	0.9925	0.9933	1.0101	0.9999	0.99997	1.0126	1.0028	1.0102	0.9997	0.99994	1.0464	1.0201
		<b>Average</b>		0.5223	1.9055		<b>Average</b>		1.1003	6.4203		<b>Average</b>		1.350	12.697

**Table 8.** The Comparison of the effectiveness factor variations under TSM and MADM [11] analytical results with numerical results by cylindrical shape pellet for various values of the Theile Modulus  $\alpha$  and various values of  $\beta$ .

$\beta$	$\alpha=0.1$					$\alpha=0.25$					$\alpha=0.5$				
	Numerical $\eta$	TSM $\eta$	MADM $\eta$	Error by TSM	Error by MAD	Numerical $\eta$	TSM $\eta$	MADM $\eta$	Error by TSM	Error by MAD	Numerical $\eta$	TSM $\eta$	MADM $\eta$	Error by TSM	Error by MAD
	$Ef$	$\eta$	$\eta$			$Ef$	$\eta$	$\eta$			$Ef$	$\eta$	$\eta$		
0.0	1.0113	1.0088	1.0088	0.2487	0.2488	0.9975	1.00227	1.0022	0.4827	0.4796	0.9792	0.9800	0.9795	0.0803	0.0348
20	21.0013	20.9988	20.9988	0.0120	0.0120	21.0078	20.9922	20.9922	0.0743	0.0743	21.0316	20.9688	20.9688	0.2987	0.2987
40	41.0013	40.9988	40.9988	0.0061	0.0061	41.0078	40.9922	40.9922	0.0381	0.0381	41.0308	40.9688	40.9688	0.1513	0.1513
60	61.0013	60.9988	60.9988	0.0041	0.0041	61.0080	60.9922	60.9922	0.0258	0.0258	61.0306	60.9688	60.9688	0.1013	0.1013
80	81.0013	80.9988	80.9988	0.0031	0.0031	81.0077	80.9922	80.9922	0.0192	0.0192	81.0313	80.9688	80.9688	0.0771	0.0771
100	101.0013	100.9988	100.9988	0.0025	0.0025	101.00759	100.9922	100.9922	0.0153	0.0153	101.0314	100.9688	100.9688	0.0620	0.0620
500	501.0013	500.9988	500.9988	0.0005	0.0005	501.00778	500.9922	500.9922	0.0031	0.0031	501.0301	500.9688	500.9688	0.0123	0.0123
		<b>Average</b>		0.0396	0.0396		<b>Average</b>		0.0941	0.0936		<b>Average</b>		0.1119	0.1054

**Table 9.** The Comparison of the Effectiveness factor variations under TSM and MADM [11] analytical results with numerical results by spherical shape pellet for various values of the Theile Modulus  $\alpha$  and various values of  $\beta$ .

$\beta$	$\alpha=0.1$					$\alpha=0.25$					$\alpha=0.5$				
	Numerical $\eta$ $E_f$	TSM $\eta$	MADM $\eta$	Error by TSM	Error by MADM	Numerical $\eta$ $E_f$	TSM $\eta$	MADM $\eta$	Error by TSM	Error by MADM	Numerical $\eta$ $E_f$	TSM $\eta$	MADM $\eta$	Error by TSM	Error by MADM
0.01	1.0110	1.0093	1.0093	0.1619	0.1619	1.0060	1.0059	1.0059	0.0143	0.0143	0.9939	0.9937	0.9937	0.0138	0.0126
20	21.0010	20.9993	20.9993	0.0079	0.0079	21.0063	20.9958	20.9958	0.0498	0.0498	21.0252	20.9833	20.9833	0.1992	0.1992
40	41.0010	40.9993	40.9993	0.0041	0.0041	41.0062	40.9958	40.9958	0.0252	0.0252	41.0246	40.9833	40.9833	0.1006	0.1006
60	61.0010	60.9993	60.9993	0.0027	0.0027	61.0062	60.9958	60.9958	0.0170	0.0170	61.0249	60.9833	60.9833	0.0681	0.0681
80	81.0010	80.9993	80.9993	0.0021	0.0021	81.0063	80.9958	80.9958	0.0129	0.0129	81.0248	80.9833	80.9833	0.0512	0.0512
100	101.0010	100.9993	100.9993	0.0016	0.0016	101.0061	100.9958	100.9958	0.0101	0.0101	101.0249	100.9833	100.9833	0.0411	0.0411
500	501.0010	500.9993	500.9993	0.0003	0.0003	501.0063	500.9958	500.9958	0.0021	0.0021	501.0250	500.9833	500.9833	0.0083	0.0083
	<b>Average</b>			0.0258	0.0258	<b>Average</b>			0.0188	0.0188	<b>Average</b>			0.0689	0.0688

## 6. CONCLUSION

In this work, a nonlinear time-independent ordinary differential equation has been solved analytically. An approximate analytical solution for substrate concentrations and their effectiveness factors were obtained by Taylor’s series method with respect to the three pellet geometries viz. planar, cylindrical and spherical. These results have also been compared with the results produced by other analytical techniques and consequently found that the Taylor series method is straightforward with a simple solution process and accurate results much closer to the numerical solutions at its fourth-order itself. This procedure can be extended without any difficulty to other boundary value problems in physical, chemical and biosciences. The essential information collected from this work is that the dimensionless substrate concentration levels have parallel tangential variations only with shifts at initial points, for the same sets of parameter values performed upon different geometrical pellets and also the analytical and numerical curves are exactly coinciding for the possible and proper values of the parameters ranging from 0.1 to 1 and ranging from 0.01 to 0.5 applicable for all the analytical techniques taken for comparison. Also, the effectiveness factor expression rendered the uniformity in the flow against the variation of the dimensionless substrate concentration under Michaelis-Menten kinetics ( $\beta$ ) and stayed independent of the Theile modulus, caused by the immobilization of the enzymes without external mass transfer resistance upon all the three geometries.

### Appendix A: Analytical solution of the given model (5) by the Taylor’s series method:

Equation (5) can be rewritten as

$$[XC''(X) + (g - 1)C'(X)](1 + \beta C(X)) - \alpha^2 XC(X) = 0 \tag{A.1}$$

In this paper, we consider a simple approach by the Taylor’s series method for solving for the dimensionless substrate concentration,  $C$ . When  $X = 1$ , we have

$$[C''(1) + (g - 1)C'(1)](1 + \beta C(1)) - \alpha^2 C(1) = 0 \tag{A.2}$$

Applying the boundary condition (7) in (A.2) and assuming that  $C'(1) = m$ , we obtain

$$[C''(1) + (g - 1)m](1 + \beta) - \alpha^2 = 0 \tag{A.3}$$

from which we obtain

$$C''(1) = \frac{\alpha^2}{1 + \beta} - (g - 1)m \tag{A.4}$$

Now differentiating (A.1) with respect to  $X$ , we get

$$XC'''(X)(1 + \beta C(X)) = -g(1 + \beta C(X))C''(X) - X\beta C''(X)C'(X) - (g - 1)\beta(C'(X))^2 + \alpha^2(XC'(X) + C(X)) \tag{A.5}$$

Again by applying the condition (7) and by our assumption, we obtain

$$C'''(1) = g(g - 1)m - \frac{(g - 1)\alpha^2}{1 + \beta} + \frac{m\alpha^2}{(1 + \beta)^2} \tag{A.6}$$

Again differentiating (A.5) with respect to  $X$ , we get

$$XC^{IV}(X)(1 + \beta C(X)) = (1 - 3g)\beta C'(X)C''(X) - (g + 1)C'''(X)(1 + \beta C(X)) - 2\beta X C'''(X)C'(X) - \beta X(C''(X))^2 + \alpha^2(2C'(X) + X C''(X)) \tag{A.7}$$

Now applying the condition (7) and the equations (A.4) and (A.6) along with our assumption, we obtain

$$C^{IV}(1) = \frac{\alpha^4}{(1 + \beta)^3} - \frac{2(g - 1)m\alpha^2}{(1 + \beta)^2} - \frac{2m^2\alpha^2\beta}{(1 + \beta)^3} + \frac{(g^2 - 1)\alpha^2}{(1 + \beta)} - g(g^2 - 1)m \tag{A.8}$$

Then by the Taylor’s series about  $X = 1$ , we have

$$C(X) = C(1) + C'(1)\frac{(X - 1)}{1!} + C''(1)\frac{(X - 1)^2}{2!} + C'''(1)\frac{(X - 1)^3}{3!} + C^{IV}(X)\frac{(X - 1)^4}{4!} + \dots \tag{A.9}$$

in which using the equations (7), (A.4), (A.6) and (A.8) along with our assumption, we obtain

$$C(X) = 1 + \frac{m(X - 1)}{1!} + \frac{(X - 1)^2}{2!} \left[ \frac{\alpha^2}{1 + \beta} - (g - 1)m \right] + \frac{(X - 1)^3}{3!} \left[ g(g - 1)m - \frac{(g - 1)\alpha^2}{1 + \beta} + \frac{m\alpha^2}{(1 + \beta)^2} \right] + \frac{(X - 1)^4}{4!} \left[ \frac{\alpha^4}{(1 + \beta)^3} - \frac{2(g - 1)m\alpha^2}{(1 + \beta)^2} - \frac{2m^2\alpha^2\beta}{(1 + \beta)^3} + \frac{(g^2 - 1)\alpha^2}{(1 + \beta)} - g(g^2 - 1)m \right] + \dots \tag{A.10}$$

Differentiating this with respect to  $X$ , we get

$$\begin{aligned}
 C'(X) = & m + (X - 1) \left[ \frac{\alpha^2}{1 + \beta} - (g - 1)m \right] \\
 & + \frac{(X - 1)^2}{2} \left[ g(g - 1)m - \frac{(g - 1)\alpha^2}{1 + \beta} + \frac{m\alpha^2}{(1 + \beta)^2} \right] \\
 & + \frac{(X - 1)^3}{6} \left[ \frac{\alpha^4}{(1 + \beta)^3} - \frac{2(g - 1)m\alpha^2}{(1 + \beta)^2} - \frac{2m^2\alpha^2\beta}{(1 + \beta)^3} + \frac{(g^2 - 1)\alpha^2}{(1 + \beta)} - g(g^2 - 1)m \right] \\
 & + \dots
 \end{aligned}
 \tag{A.11}$$

where  $m$  is obtained by using the boundary condition (6) in (A.11) as follows.

By condition (6), we have

$$\begin{aligned}
 0 = & 2\alpha^2\beta m^2 + [(g^3 + 3g^2 + 2g)(1 + \beta)^3 + (2g + 1)\alpha^2(1 + \beta)]m \\
 & - \alpha^4 - [g^2 + 3g + 2]\alpha^2(1 + \beta)^2
 \end{aligned}
 \tag{A.12}$$

Substituting various possible values of the parameters  $\alpha$  and  $\beta$ , the  $m$  values have been collected as given in the Tables 1, 3 and 5 corresponding to the geometries planar, cylindrical and spherical by replacing the pellet shape factor values such that  $g = 1$ ,  $g = 2$  and  $g = 3$  respectively in (A.12). The geometry wise dimensionless concentration profile expressions are given by the equations (18), (21) and (24) for planar, cylindrical and spherical respectively.

### Appendix B: MATLAB Coding

```

function sivakumar
m = 1;
x = linspace(0,1);
t = linspace(0,1000);
sol = pdepe(m,@pdex4pde,@pdex4ic,@pdex4bc,x,t);
u1 = sol(:,:,1);
%u2 = sol(:,:,2);
%figure
plot(x, u1(end,:),'-')
%title('u1(x, t)')
%xlabel('Distance x')
%ylabel('u1(x,t)')
%figure
%plot(x, u2(end,:),'b')
%title('u2(x, t)')
%figure
% -----
function [c,f,s] = pdex4pde(~,~,u,DuDx)
al=10.0;be=1000.0; %These parameter values are used in Fig.2
c = [1;1];
f = [1;1].* DuDx;
F1=-(al.^2)*u(1)/(1+(be*u(1)));
F2=-(al.^2)*u(2)/(1+be*u(2));
    
```

```

s = [F1;F2];
% -----
function u0 = pdex4ic(~)
u0 = [1; 0];
% -----
function [pl,ql,pr,qr] = pdex4bc(~,~,~,ur,~)
%bi=10.0;
pl = [0;0];
ql = [1;1];
pr = [ur(1)-1;0];
qr = [0;1];
%qr = [0; bi*(1-ur(2))];

```

## Declarations

### FUNDING

No funding was received to assist with the preparation of this manuscript.

### CONFLICTS OF INTEREST/COMPETING INTERESTS

The authors declare that there is no conflict of interest.

### AVAILABILITY OF DATA AND MATERIAL

Data sharing not applicable to this article as no datasets were generated or analysed during the current study.

### ACKNOWLEDGEMENT

The Authors are very much grateful to the management, SRM Institute of Science and Technology, Kattankulathur, for their continuous support and encouragement.

## References

1. L. Goldstein. *Methods in Enzymology.*, 44 (1976) 397.
2. T. Kobayashi and K. J. Laidler. *Biochim. Biophys. Acta.*, 302 (1973) 1.
3. A. Kheirilomoom, S. Katoh, E. Sada, and K. Yoshida. *Biotechnol. Bioeng.*, 37, (1991) 809.
4. S. Gondo, S. Isayama and K. Kusunoki. *Biotechnol. Bioeng.*, 17, (1975) 423.
5. D. J. Fink, T.Y. Na, and J.S. Schultz. *Biotechnol. Bioeng.*, 15, (1973) 879.
6. S.A. Miresghhi, A. Kheirilomoom and F. Khorasheh. *Scientia Iranica.* 3(3) (2001) 189.
7. J.Y. Houn, H. Yu, K.C. Chen, and C. Tiu. *Biotechnol. Bioeng.*, 41 (1993) 451.
8. I.H. Segel, *Enzyme Kinetics*, Wiley, New York (1993).
9. F. Shirraishi, *Int. Chem. Engg.*, 32 (1992) 140.
10. R. Senthamarai, and T.N. Saibavani. *J. Phys. Conf. Ser.*, 1000 (2018) 1.
11. K. Narayanan, V. Meena, L. Rajendran, J. Gao and S. Subbiah. *Applied and Computational Math.*, 6 (3) (2017) 143.
12. L. Weise, G. Valentin, A. Storck, *J. Appl. Electrochem.*, 16 (1986) 851.
13. E. Miletics and G. Molnarka. *J. Comput. Methods Sci. Eng.*, 4 (2004) 105.
14. R. Usha Rani and L. Rajendran. *Chem. Phys. Lett.*, 754 (2020) 1.
15. K. C. Chen and C. M. Chang. *Enzyme Microb. Technol.*, 6 (1984) 359.
16. M. Matinfar, M. Ghasemi. *Int. J. Numer. Methods Heat Fluid Flow.*, 23 (2013) 520.
17. P. Rentrop. *Numer. Math.*, 31 (1978) 359.

18. A. M. Wazwaz. *Appl. Math. Comp.*, 102 (1) (1999) 77.
19. R. Rach, J. S. Duan, A. M. Wazwaz. *Chem. Engg. Comm.*, 202 (8), (2015) 1081.
20. B. Manimegalai, M. E. G. Lyons and L. Rajendran. *J. Electroanal. Chem.*, 880 (2021) 114921.
21. G. Sivashankari and R. Senthamarai. *AIP Conf. Proceedings*, 2277 (2020) 0025515.
22. M. Sivakumar and R. Senthamarai. *AIP Conf. Proceedings*, 2277 (2020) 130009.
23. M. Nivethitha and R. Senthamarai. *AIP Conf. Proceedings*, 2277(2020) 210005.
24. T. Vijayalakshmi and R. Senthamarai, *Int. J. Adv. Sci. and Tech.*, 29(6) (2020) 2853.
25. R. Senthamarai and R. Jana Ranjani. *J. Phys. Conf. Ser.*, 1000 (2018) 012138.
26. S. Muthukaruppan and R. Senthamarai and L. Rajendran. *J. Electroanal. Chem.*, 7 (2012) 9122.

© 2022 The Authors. Published by ESG ([www.electrochemsci.org](http://www.electrochemsci.org)). This article is an open access article distributed under the terms and conditions of the Creative Commons Attribution license (<http://creativecommons.org/licenses/by/4.0/>).